Supplemental Information

Methods

Cell Lines

WT (C57BL/6) or *Polm*$^{-/-}$ murine fibroblast cells (generously provided by Dr. L. Blanco) were derived from E14.5-d embryos and immortalized by the introduction of SV-40 large T-antigen as described previously (*24*). The ts-AbMLV pre-B cells were a generous gift from Dr. Y. Chang (Arizona State University). These lines and variants described below were confirmed to be free of mycoplasma contamination by PCR (*25*); cell lines were additionally selected at random for third party validation of PCR results using Hoechst staining (*26*). Variants of MEFs and pre-B cell lines with frameshift mutations in Exon 2 of the *Rnaseh2a* gene or Exon 1 of the *Polm* gene were generated by transient expression of nickase Cas9 D10A and a pair sgRNAs (Table S2). Cell lines were engineered to express appropriate mouse cDNAs for Myc-tagged Pol μ, TdT, or RNaseH2A by infection with retrovirus derived from pBabe-puro constructs for Pol μ and TdT, or infection with lentivirus derived from a pLX302 construct (Addgene no. 25896) for RNaseH2A. RNaseH2A complementation was performed on bulk infected cells that were selected in puromycin for 5 days; all other cell lines were sub-cloned by limiting dilution and verified by western blot analysis and allele sequencing (where applicable). Wild-type and LIG4-deficient HCT116 cells were a gift from Dr. Eric Hendrickson. Western blots were performed using standard techniques and antibodies against murine RNaseH2A (ProSci, 4979), Actin (Sigma, A2066), TdT (Sigma, 14.9739.80), or the Myc affinity tag (Santa Cruz, sc409E10). MEF and HCT116 cells were maintained in DMEM supplemented with 10% (vol/vol) FBS (Sigma), 5 mM N-acetyl-L-cysteine (Sigma), 2 mM L-glutamine (Gibco), 100U/ml penicillin, and (in variant lines expressing puromycin resistance markers) 2 μg/mL puromycin, at 37°C and

5% CO_2. The ts-AbMLV cell lines were maintained in RPMI 1640 (Corning) supplemented with 10% (vol/vol) FBS (Sigma), 2 mM L-glutamine (Gibco), 55 μM 2-mercaptoethanol (Gibco), 100U/ml penicillin, and (in variant lines expressing puromycin resistance markers) 2 μg/mL puromycin, at 33°C and 5% CO_2.

Statistical methods. Means were compared by ANOVA (Prism, Graphpad) to control samples, and p values corrected for multiple comparisons.

Double strand break repair assays

Substrates described in Fig. 1 were generated by PCR amplification of a common 285-bp DNA segment with primer pairs containing embedded restriction enzyme digest sites chosen to generate the desired end structures (Table S2). Substrates were digested, purified by agarose gel electrophoresis, and purified substrate recovered using the QiaQuick gel-extraction kit (Qiagen). Substrates described in Fig. 3 were assembled by ligation of ~15 bp double-stranded DNA caps (oligonucleotide pairs annealed to generate gaps in Table S2) containing the desired overhang sequence to a 280 bp core fragment digested with BsaI-HF (New England Biolabs), with the caps in 3 fold excess. Substrates were then purified using a QiaQuick PCR purification kit (Qiagen), and resolved on a native acrylamide gel to ensure substrates preparations were free of detectable unappended core and excess cap.

Extrachromosomal substrate electroporations were carried out using the NEON transfection system (Invitrogen) with 20 ng of substrate, 600 ng pMAX-GFP carrier plasmid, and 2×10^5 cells by a 1350 V, 30 ms pulse in a 10 μl chamber. 5 seconds after, cells were decanted into pre-warmed 37°C Hank's Buffered Salt Solution (Gibco) supplemented with 1 mM $MgCl_2$ and Benzonase Nuclease (Sigma) for the indicated amount of time. DNA was harvested using a

QiaAmp DNA mini kit (Qiagen). NHEJ products were quantified by a qPCR specific for head-to-tail ligation (Table 1), and total transfected substrate and product (Input) quantified by a qPCR specific for a segment of the substrate (Fig. S5G).

V(D)J recombination was induced by culture of SP9 or SP9 variants at 40^{o}C for 24 hours. Comparison of levels of induced V(D)J recombination (Fig. S3E) were made after first normalizing for input genomes using a qPCR assay specific to a locus located 28kbp 5' of *Rosa26* (Table S2).

Rosa26 locus-targeting Cas9 ribonucleoproteins (RNPs) were assembled from purified Cas9 (derived from Addgene #69090), and annealed Alt-R modified crRNA (Table S2) and trcrRNA (IDT). The Cas9-sgRosa26 RNP complex was introduced at 1.8 μM into 2×10^6 cells and a 100 uL chamber using a 1350 V, 30 ms pulse and incubated at 37°C before cell harvesting and purification of genomic DNA (QiaAmp DNA mini kit). For experiments involving nucleotide electroporation into cells the transfection mixture was supplemented with either 10 mM rGTP, 10 mM dGTP, (dNTPs from New England Biolabs) or an equivalent concentration of the relevant monovalent cation (Na^+; "none"). TdT-dependent additions were assessed by qPCR using primers that amplify only the class of Cas9-incuded break repair products that possessed n deletion downstream of the cut site, and two or more added Gs. Comparison of +GG product amounts over time (Fig. S4C and S4D) were made after normalizing genome amounts using a qPCR specific for a locus 28 kbp 5' of *Rosa26* (Table S2). Mutations in CRISPR-Cas9 products were assessed by amplifying the targeted locus and either by restriction digest of products with XbaI (does not cleave products with deletions upstream of the Cas9-sgRosa26 RNP cut site), or by Sanger sequencing and Tracking of Indels by DEcomposition (TIDE) (*27*).

In vitro NHEJ assays were initiated by incubating 2 nM DSB substrates with either NHEJ proteins (25 nM Ku, 40 nM XLF, and 40 nM XRCC4-LIG4) or T4 DNA ligase in a buffer with 25 mM Tris pH 7.5, 100 uM EDTA, 1 mM DTT, 1 mM MgCl, 100 uM ATP, 150 mM KCl, 7.5% polyethelene glycol 3000, and 100 ng of supercoiled plasmid DNA. Reactions were carried out for 10 minutes at 37 C. stopped with 0.1% SDS and 20 mM EDTA, and products quantified by qPCR.

Repair product analysis

Quantitative ribonucleotide detection experiments described in Fig. 1B, 2B, and 2D were performed by splitting experimental samples into two aliquots, and either mock treating a sample aliquot or treating a sample aliquot with 2.5 units of RNaseHII (New England Biolabs) at 37 C for 16 hours in Thermopol buffer (New England Biolabs). These conditions were sufficient to cleave to completion sites of embedded ribonucleotides regardless of opposite strand structure, with no obvious digestion of DNA-only controls. As an alternative method of ribonucleotide cleavage, samples in Fig. S2A were treated with 300 mM NaOH for 2 hours at 55 ºC (or mock treated with 300 mM NaCl) and neutralized by a 10x dilution into 65 mM Tris-HCl buffer (pH 8.0). Restriction enzymes that cut outside the amplicons (NlaIII and MseI for Rosa26 samples, and HaeIII and MseI for substrate samples) were also included to ensure the initial denaturation of template duplexes (and thus amplification) occurred with equal efficiency when comparing RNaseHII and mock treated samples. The fraction of NHEJ product with embedded ribonucleotide (%ribo.) was then determined by comparison of product remaining after cleavage at embedded ribonucleotides (ribonucleotide cleaved sample), relative to total product (mock treated sample)(Fig. S1B). Normalization to total product corrects for differences in input and

NHEJ product accumulation, and allows for direct comparison of the amount of ribonucleotides in NHEJ products at different timepoints and in different transfections.

Most experiments (Fig. 1B, 2B, 2D, S4E, S4F) assessed %ribo using real time PCR assays (qPCRs), a QuantStudio 6 System (Applied Biosystems), primers that amplify head-to-tail junctions (Table S2), and VeriQuest Probe qPCR Master Mix (Affymetrix). These qPCR assays were linearly response to increasing template over the ranges we use (Fig S1A, S3A, S4B). We additionally assessed the accuracy of our method for measuring ribonucleotides (Fig. S1C). We used two mock NHEJ products - one with embedded ribonucleotides, and one without - and mixed them, with increasing proportion of products with embedded RNA to generate "input % ribo." samples with 0, 12.5, 37, 50, and 100% product with embedded ribonucleotides. These mixtures were diluted into an appropriate excess of genomic DNA to generate samples with a NHEJ product:background genomic DNA ratio equivalent to samples from cellular experiments. The %ribo. in products was determined in triplicate for each mixture as described above (measured % ribo.), then compared to the input% ribo. in each sample to generate the standard curve in Fig. S1C. Analysis of the standard curve by linear regression (Prism, Graphpad) indicated there was no significant loss of pure DNA products after digestion at embedded ribonucleotides (y intercept=-1.2%, +/-1.0). There was also a good linear response of measured % ribo. to increasing input % ribo. (slope=1.0, +/-0.02, R^2=1.0), indicating the amplification efficiency for ribonucleotide-embedded products is not significantly different from pure DNA products. We estimate the practical minimum detection limit was approximately 12.5% input ribo.

For remaining experiments (Figure 1E, S2), repair products were mock treated or treating with ribonucleotide cleaving agent before amplification, as above. Together with experiments

described in Fig. 3 and Table 1, products were then amplified with a Cy5-labelled primer, and amplified products further characterized by digestion after amplification with restriction enzymes diagnostic for specific products (Table 1; NsiI for G3' and CG3', SalI for CAG3', AatII for CGCAG3', and FspI for TTTTTTTTGC3'). Digestion products were resolved on a 5% non-denaturing polyacrylamide gel, visualized using a Typhoon Imager (GE Healthcare), and quantified using ImageJ softward. %ribo. in Fig. 1E and S2 was determined by comparing the intensity of restriction enzyme sensitive bands from samples amplified after ribonucleotide cleavage, vs. samples amplified after mock cleavage. % direct joining in Fig. 3 and Table 1 was determined by comparing intensities of restriction enzyme sensitive bands vs. intensity of all other (restriction enzyme resistant) species.

Next-generation Sequencing

Template DNA for each sequencing library (~5×10^5 input molecules for substrate experiments; 2 x 10^4 for *Rosa26* locus experiments) was amplified using Phusion DNA polymerase (New England Biolabs) and PCR primers with six-nucleotide index sequences appended to their 5′-ends (Table S2). Amplified DNA was 5′phosphorylated with T4 Polynucleotide kinase then treated with Klenow exo- to add dA to the 3′ termini (New England Biolabs). Sequencing adapters for paired-end reads were appended to the amplicons by treatment with T4 DNA ligase, and free adapter removed by agarose gel purification. After a final enrichment PCR amplification the products were purified by Agencourt AMPure XP beads (Beckman Coulter). Libraries were submitted for a 2 × 150-bp sequencing run (MiSeq; Illumina) with a PhiX174 DNA "spike". Data analysis with Genomics workbench v7.5.1 (CLC-Bio, Qiagen) and Microsoft Excel was carried out as described(*15*).

Supplementary Figure Legends

Fig. S1: Assays and cell lines for assessing ribonucleotide content during NHEJ.

(A) A serial dilution of an oligonucleotide model repair product from the extrachromosomal NHEJ assay (Fig. 1) was used as a template in a qPCR reaction. Mean qualification cycle (Cq) from 3 independent experiments is plotted with error bars representing sd. **(B)** Schematic of RNA detection assay: repair products are either mock digested or digested with RNase HII to destroy RNA-containing products, and then % ribo. is calculated from the difference in qPCR Cq values. **(C)** Model NHEJ products, one containing a single embedded ribonucleotide, and one containing a pure DNA NHEJ products were mixed at various proportions (input % ribo.), and diluted into genomic DNA at a target to genomic DNA ratio equivalent to experimental conditions. These mixtures were mock or RNaseHII digested before qPCR as described in methods. Mean detected ribonucleotides (measured % ribo.) from 3 experiments is plotted with error bars representing sd. **(D)** Extrachromosomal substrate assay was performed as in Fig. 1A for the indicated amounts of time. Mean repair efficiency of 3 independent transfections is plotted with error bars representing sd. **(E-G)** Western blots were performed using primary antibodies specific to the indicated antigen (Myc, TdT, Actin or RNaseH2A) in the indicated MEF cell lines. **(H)** Substrate assay was performed as in Fig. 1B for 20 minutes, and % ribo. was determined in wild-type MEFs, *Rnaseh2a*$^{-/-}$ MEFs, and *Rnaseh2a*$^{-/-}$ MEFs complemented by lentiviral delivery of *RNaseH2A*. Error bars represent sd and means were assessed for significant difference from wild-type by one-way ANOVA as not significant (ns) or $p<0.001$ (***).

Fig. S2: Detection of ribonucleotides in cellular NHEJ products.

(A-B) Repair products were recovered after 1 minute as in Fig. 1E. **(A)** %ribo. determined by comparison of samples treated with alkali and heat to mock treated. **(B)** %ribo. of +G product determined as in Fig. 1E. Ribonucleotide detection is shown as the mean ± sd of 3 independent transfections.

Fig. S3: Cell lines and methods for detecting ribonucleotides in V(D)J recombination.

(A) A model amplicon of V(D)J recombination products at the murine V_K locus was amplified by qPCR. Data represent the mean quantitation cycle (Cq) from 3 independent experiments and error bars represent the sd. **(B-D)** Western blots were performed against the indicated affinity tag and murine proteins (Myc, TdT, Actin or RNaseH2A) in the indicated SP9 cell lines. **(E)** V(D)J recombination was induced for 24 hours in SP9 pre-B cells of the indicated genotypes and induction was measured by qPCR across the VJ_K junction. All data points and the mean induction level are shown. Experiments were compared to the wild type parental line by ANOVA with p values corrected for multiple comparisons, and are reported as ns (no significant difference from wild type parental line), or * (significantly different from parental line, $p<0.05$).

Fig. S4: Ribo-NHEJ facilitates genome engineering.

(A) Genomic DNA was harvested from wild-type or *Polm*$^{-/-}$ MEFs targeted with Cas9-sgRosa26 and repair products were analyzed by high-throughput sequencing. Data represent the difference in mean frequencies for three independent transfections for recovered products of the indicated lengths after comparing products from wild-type vs. *Polm*$^{-/-}$ MEFs. **(B)** A serial dilution of a model amplicon of the TdT-dependent +GG repair CRISPR repair product was used as a template for qPCR. Data represent the mean Cq from 3 independent experiments and error bars represent the sd. **(C-F)** CRISPR break repair assay was performed as described in Fig. 2C and

(C) +GG repair products were assessed 0 or 72 hours after introduction of Cas9 RNP, with or without TdT expression. Results from triplicate transfections are shown, and error bars represent the sd from the mean. Means were tested by one-way ANOVA as significantly different from 0 hour timepoint at $p < 0.001$ (***). **(D)** Accumulation of +GG repair products over the indicated amounts of time using TDT-expressing *RnaseH2a*$^{-/-}$ MEF cells. Mean product recovery efficiency, relative to 72 hours, for 3 independent transfections is plotted with error bars representing sd. **(E-F)** Data represent the mean ribonucleotide detection in 3 independent experiments and error bars represent the sd. for **(E)** %ribo. in +GG products recovered after 1 hour from TDT-expressing MEF cells either proficient or deficient in *Rnaseh2a*, or **(F)** %ribo. detected at an uncut genomic control locus upstream of *Rosa26,* or in *Rosa26* +GG products as in Fig. 2D.

Fig. S5: Ribonucleotides enable direct ligation of complex end structures.

(A) Substrate with 3'GA overhangs was introduced into *Polm*$^{-/-}$ and complemented MEFs. The mean fraction of repair products ligated after addition of a single complementary C was quantified by restriction digest. Data represent the means of three independent experiments, +/- sd. **(B)** The indicated NHEJ substrate was introduced into cells either proficient or deficient in LIG4. Repair products were amplified by qPCR. All data points and the mean repair efficiency are shown. Mean recovery was tested by t-test as significantly different between wild-type and *LIG4*$^{-/-}$ cells at $p < 0.001$ (***). **(C)** Structural models and sugar puckers of substrates used in Fig. 3C to assess the mechanism by which ribonucleotides benefit complex end ligation. **(D)** *in vitro* ligation reactions were performed on the indicated substrate using either NHEJ proteins (Ku, XLF, XRCC4, LIG4) or T4 DNA ligase. Ligation was quantified by qPCR and data represent the mean ligation stimulation conferred by a ribonucleotide, from 3 independent

ligation reactions with error bars representing sd. Mean ribo stimulation was tested by t-test as significantly different between LIG4 and T4 ligase at $p < 0.01$ (**). **(E-F)** Substrates with complex ends and either a terminal ribonucleotide or deoxynucleotide were introduced into polymerase-deficient MEF cells and repair product structures were analyzed by high throughput sequencing. **(E)** Repair products were categorized as either directly joined (orange) or deletion products (gray). The area of the rC pie graph was made proportional to the mean joining efficiency for this substrate relative to the joining efficiency for the dC substrate, as determined by qPCR. **(F)** The deletion size was determined for each recovered product and averaged for rC vs. dC substrates. **(G)** Indicated substrates were introduced into MEF cells as in Table 1. The total amount of substrate introduced into cells was quantified by qPCR. Data represent the means of 3 independent transfections and error bars represent sd.

Fig. S6: Effect of nucleotide triphosphate supplementation on repair of Cas9 breaks

(A-C) *Rosa26*-targeted Cas9 RNP was introduced into MEF cells as in Fig. 2 C-D, along with nucleotide triphosphates as indicated. Genomic DNA was harvested 1 hour after transfection. **(A)** The targeted locus was amplified by PCR and digested with XbaI to distinguish products with deletions of upstream flanking DNA (XbaI resistant) from all remaining products. Mutated products were quantified as the mean ratio of XbaI-resistant amplicon in 3 independent transfections with error bars representing s.d. Mean XbaI-sensitivity was tested by one-way ANOVA as significantly different from sample with no nucleotide added at $p < 0.001$ (***) or not significant (ns). **(B)** Products of uncut control and repair after Cas9 cleavage were amplified and Sanger sequenced directly, followed by assessment of deviation from the uncut control using Tracking of Indels by Decomposition (TIDE) (*27*). Indels were quantified in this manner for 3 independent transfections for each experiment, with error bars representing the sd. Mean indel

frequency was tested by two-way ANOVA as significantly different from sample with no nucleotide added at $p < 0.001$ (***) or not significant (ns). **(C)** TdT-specific +GG product was detected and analyzed as in Fig. 2C-D for 3 independent transfections for each experiment, with error bars representing the sd.Mean +GG product recovery was tested by t-test as significantly different between samples with no nucleotide added and samples with ara-GTP added at $p < 0.001$ (***).

Supplementary Tables

Table S1. Frequencies of 10 most common Cas9-sgRosa26 repair products in MEF cells expressing TdT

5’ flank TCTTTCTAGA	Insertion	3’ flank AGATGGGCGG	Frequency % (sd) +TdT (sd)	-TdT (sd)
TCTTTCTAGA	GG	AGATGGGCGG	13 (1.1)	0.4 (0.16)
TCTTTCTAGA	CC	AGATGGGCGG	5.2 (0.15)	0.2 (0.04)
TCTTTCTAG-		AGATGGGCGG	4.2 (1.0)	32 (1.7)
TCTTTCTAGA	G	AGATGGGCGG	4.4 (0.52)	0.3 (0.05)
TCTTTCTAGA	A	AGATGGGCGG	3.3(0.31)	5.5 (0.51)
TCTTTCTAGA		AGATGGGCGG	2.9 (0.15)	8.9 (3.5)
TCTTTCTAG-	GG	AGATGGGCGG	2.4 (0.20)	0.1 (.007)
TCTTTCT---		AGATGGGCGG	1.9 (0.61)	12.3 (0.6)
TCTTTCTAGA	AA	AGATGGGCGG	1.7 (0.02)	0.09 (0.02)
TCTTTCTAGA	GGG	AGATGGGCGG	1.6 (0.01)	0.05 (0.02)

Table S2. Sequences of DNA Reagents

Substrate Construction Oligonucleotides (5’ to 3’) *<u>*Italics*</u> = deoxy/ribo	
Core	
CAAGTGGTCTCAGACTGGCTACCCTGCTTCTTTGAGCATTTCTGAAACTATCACTT GTGTTTATTATTACACTGGCATTCATTCTCCAGAGAACATGTCTAGCCTATTCCCA GCTTTGCTTACGGAGTTACTCTGTATCTTTGCCTTGGAGAGTGCCAGAATCTGGTT TCAGAGTAAGATTTTATACATCATTTTTAGACATAGAAGCCACAGACATAGACAA CGGAAGAAAGAGACTTTGGATTCTACTTACGTTTGATTTCCCTGACGGAGACCTCG GC	
Substrates Generated by PCR and Restriction Digest	
G Substrate Forward	GTACCAAGTGGACCACATGTCTTAGCTGTA TAGTCAGGGA
G Substrate Reverse	GTACGCCGCCGACGCCATGTCACACCCATC TCAGACTGGC
C Substrate Forward	CAAGTGGACCAGACGTCTTAGCTGTATAGT CAGGGAAATC
C Substrate Reverse	CCGCCGACGCGACGTCACACCCATCTCAGA CTGGCTACCC
Substrates Generated by Cap Annealing and Ligation	
CG / CG Left Cap Top Strand	AGTCTGAGATGGGTGTCATG*<u>C</u>*
CG / CG Left Cap Bottom Strand	ATGACACCCATCTCA
CG / CG Right Cap Top Strand	TGACTATACAGCTAAGGTCATGC
CG / CG Right Cap Bottom Strand	ATGACCTTAGCTGTATA
CAG / AG Left Cap Top Strand	AGTCTGAGATGGGTGTGTCGA*<u>C</u>*
CAG / AG Left Cap Bottom Strand	GACACACCCATCTCA
CAG / AG Right Cap Top Strand	TGACTATACAGCTAAGGTGTCGA
CAG / AG Right Cap Bottom Strand	GACACCTTAGCTGTATA
CGCAG / GCAG Left Cap Top Strand	AGTCTGAGATGGGTGCCACGACG*<u>C</u>*
CGCAG / GCAG Left Cap Bottom Strand	GTGGCACCCATCTCA
CGCAG / GCAG Right Cap Top Strand	TGACTATACAGCTAAGCCCACGACG
CGCAG / GCAG Right Cap Bottom Strand	GTGGGCTTAGCTGTATA
CGTTTTTTTT / G Left Cap Top Strand	AGTCTGAGATGGGTGTGCCATTTTTTTTG*<u>C</u>*
CGTTTTTTTT / G Left Cap Bottom Strand	TGGCACACCCATCTCA
CGTTTTTTTT / G Right Cap Top Strand	TGACTATACAGCTAAGTGCG
CGTTTTTTTT / G Right Cap Bottom Strand	GCACTTAGCTGTATA
PCR Primer Oligonucleotides	
PCR-Digest assay to detect extrachromosomal substrate repair products	
Forward Primer	CTTACGTTTGATTTCCCTGACTATACAG
Reverse Primer	GCAGGGTAGCCAGTCTGAGATG
TaqMan assay to measure repair efficiency of extrachromosomal substrates	

Forward Primer	CCACAGACATAGACAACGGAAG
Reverse Primer	ACACAAGTGATAGTTTCAGAAATGC
Probe (FAM-ZEN)	TCTCAGACTGGCTACCCTGCTTCT
TaqMan assay for V(D)J recombination products at murine IgK locus	
Forward Primer	GGTTTAGTGGCAGTGGGTCTGGGAC
Reverse Primer	CTTTGCCTTGGAGAGTGCCAGAATC
Probe (FAM-ZEN)	AGCCACAGACATAGACAACGGAAGA
TaqMan assay for TdT-dependent CRISPR repair product (+GG)	
Forward Primer	TCAGTTGGGCTGTTTTGGAG
Reverse Primer	GAAGACTCCCGCCCATCACC
Probe (FAM-ZEN)	TCAGTAAGGGAGCTGCAGTGGAGTA
TaqMan assay 28412 bp upstream of Rosa26 locus to quantify number of genomes	
Forward Primer	GGGAAGTGAGAGAGAAACTGAAG
Reverse Primer	AAACCTGAGCCAGACTTTCC
Probe (VIC)	TCAGCAAAGACCGCGGAAAGATCT
High-throughput sequencing library preparation	
Substrate Forward Primer	(index)cttacgtttgatttccctgactatacag
Substrate Reverse Primer	(INDEX)gcagggtagccagtctgagatg
Adapter Top Strand	GATCGGAAGAGCGGTTCAGCAGGAATGCCGAG
Adapter Bottom Strand	ACACTCTTTCCCTACACGACGCTCTTCCGATCT
Enrichment Forward Primer	AATGATACGGCGACCACCGAGATCTACACTCTTTCCCTACACGACGCTCTTCCGATCT
Enrichment Reverse Primer	CAAGCAGAAGACGGCATACGAGATCGGTCTCGGCATTCCTGCTGAACCGCTCTTCCGATCT
SYBR Green assay to detect unrepaired and repaired extrachromosomal substrates	
Forward Primer	GGCACTCTCCAAGGCAAAGA
Reverse Primer	ACATGTCTAGCCTATTCCCGGCTT
PCR Primers to amplify targeted *Rosa26* locus for product structure analysis	
Forward Primer	GGCGGATCACAAGCAATAAT
Reverse Primer	TCAGTTGGGCTGTTTTGGAG
sgRNA Targets *lower case = PAM	
Mouse *Rnaseh2a* Target Guide 1	GCCACTTTCCCCACGGGCCTagg
Mouse *Rnaseh2a* Target Guide 2	TTTCTGCAGCCTGGGCAGACagg
Mouse *Polm* Target Guide 1	CAAGGTAGATGGCCACATCCggg
Mouse *Polm* Target Guide 2	CGCGAATGGGCCGCAGCCGCcgg
Mouse *Rosa26* Target Guide	ACTCCAGTCTTTCTAGAAGAtgg

Fig. S1

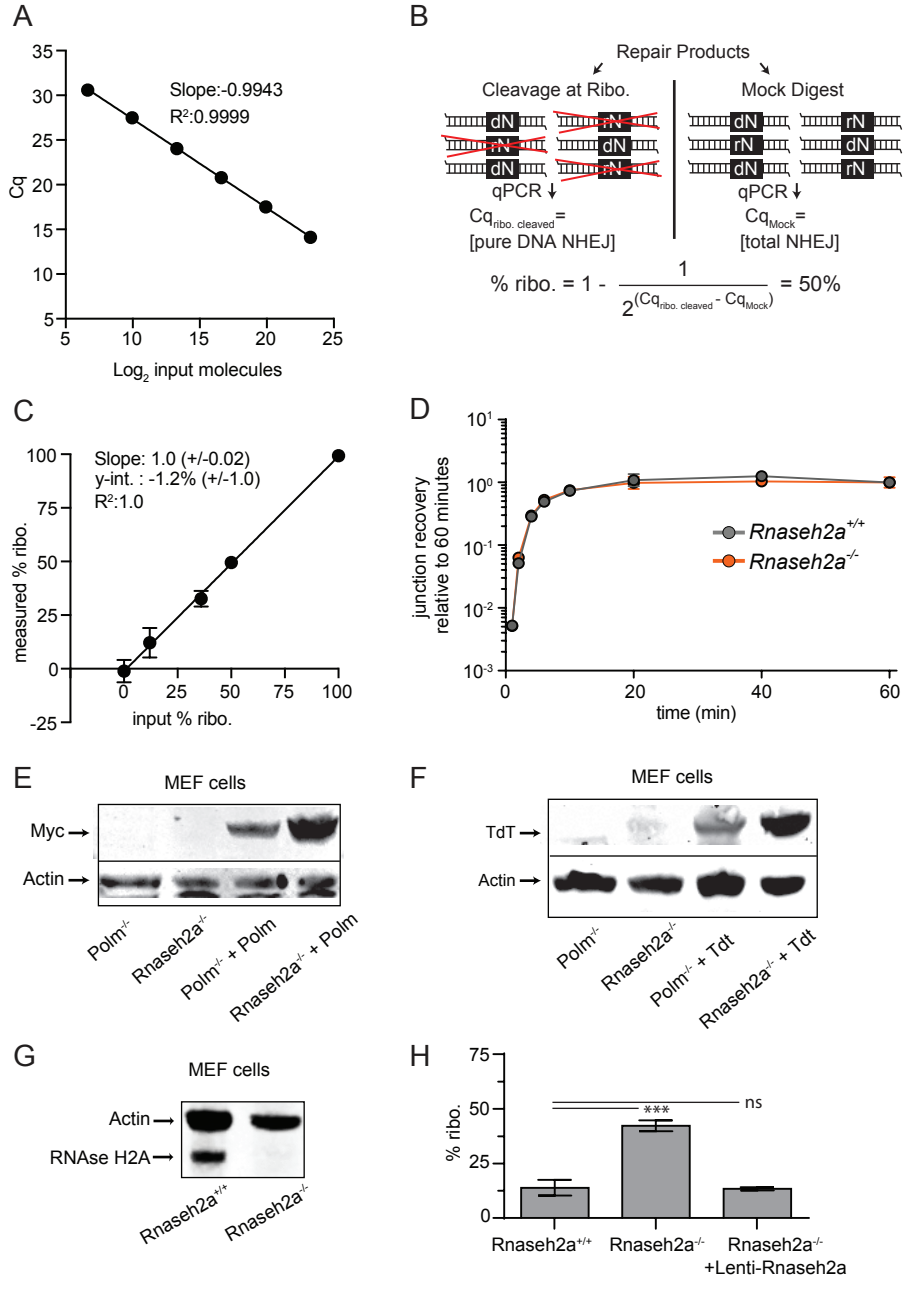
A
Slope:-0.9943
R²:0.9999
Cq
Log2 input molecules
B
Repair Products
Cleavage at Ribo.
Mock Digest
dN
rN
qPCR
Cq ribo. cleaved = [pure DNA NHEJ]
Cq Mock = [total NHEJ]
% ribo. = 1 - 1 / 2^(Cq ribo. cleaved - Cq Mock) = 50%
C
Slope: 1.0 (+/-0.02)
y-int. : -1.2% (+/-1.0)
R²:1.0
measured % ribo.
input % ribo.
D
junction recovery relative to 60 minutes
time (min)
Rnaseh2a+/+
Rnaseh2a-/-
E
MEF cells
Myc
Actin
Polm-/-
Rnaseh2a-/-
Polm-/- + Polm
Rnaseh2a-/- + Polm
F
MEF cells
TdT
Actin
Polm-/-
Rnaseh2a-/-
Polm-/- + Tdt
Rnaseh2a-/- + Tdt
G
MEF cells
Actin
RNAse H2A
Rnaseh2a+/+
Rnaseh2a-/-
H
% ribo.
***
ns
Rnaseh2a+/+
Rnaseh2a-/-
Rnaseh2a-/- +Lenti-Rnaseh2a

Fig. S2

A

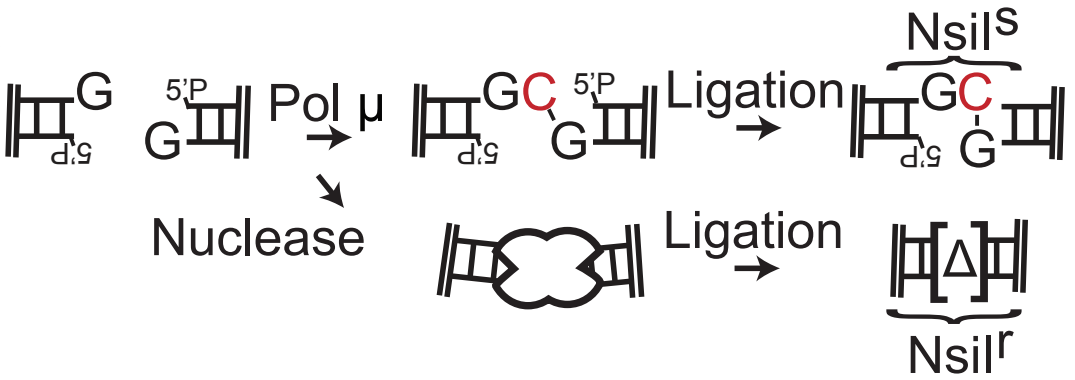
NsilS
Pol μ
Nuclease
Ligation
Ligation
NsilR

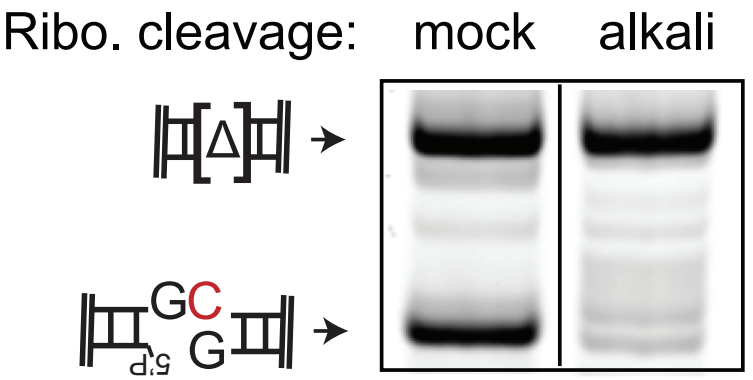
Ribo. cleavage:
mock
alkali

B

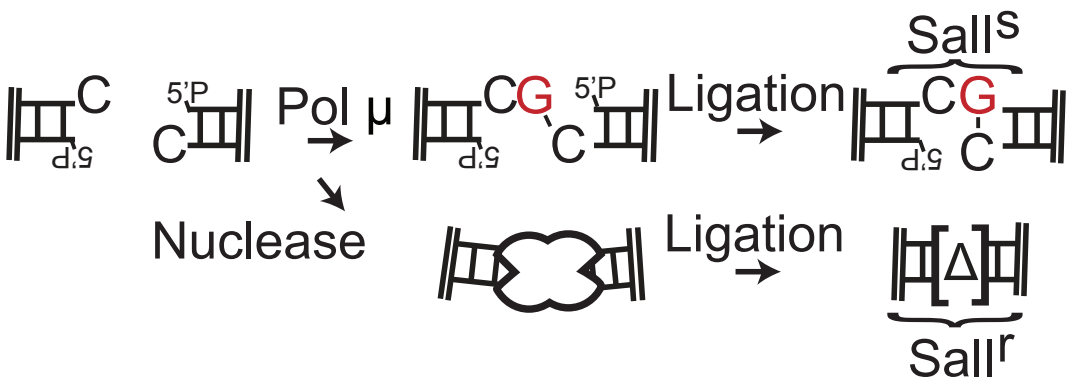
SalIS
Pol μ
Nuclease
Ligation
Ligation
SalIR

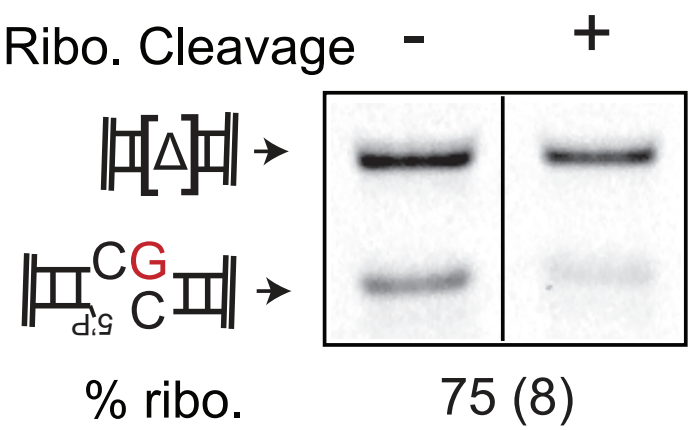
Ribo. Cleavage
-
+
% ribo.
75 (8)

Fig. S3

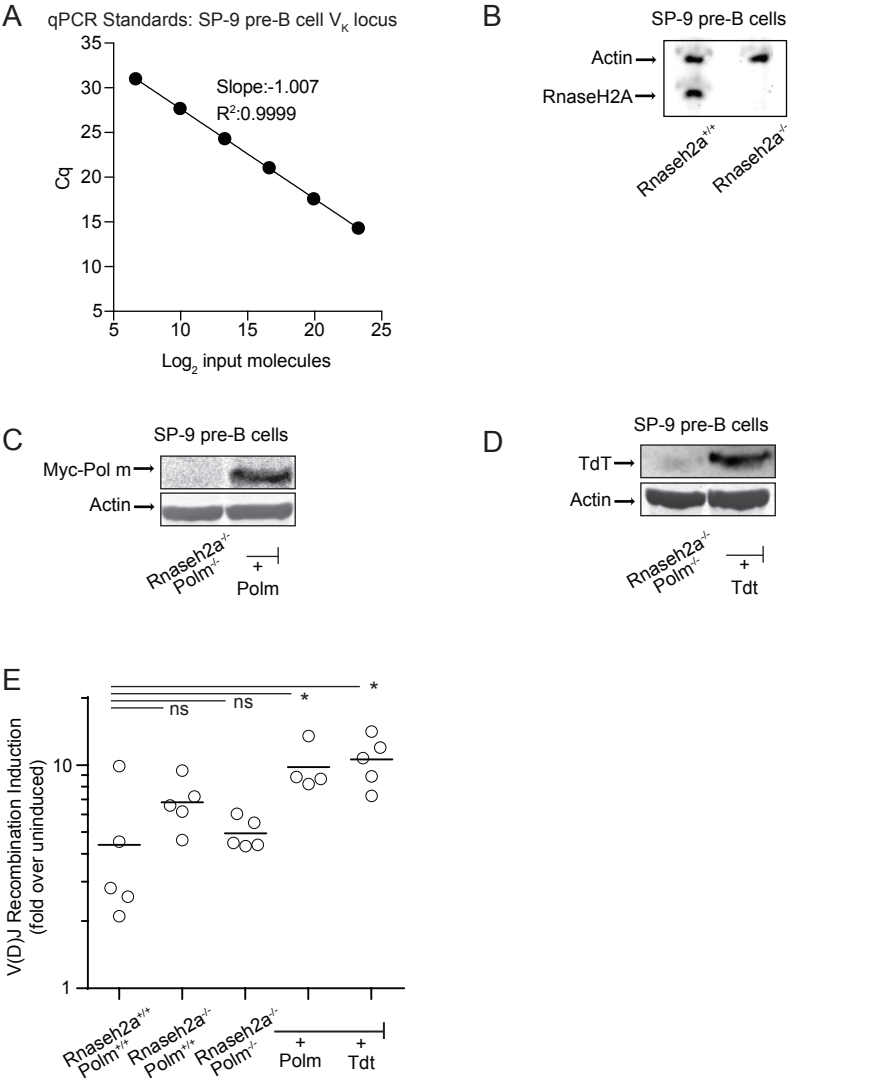
A
qPCR Standards: SP-9 pre-B cell V_K locus
Slope:-1.007
R^2:0.9999
Cq
Log_2 input molecules
B
SP-9 pre-B cells
Actin
RnaseH2A
Rnaseh2a+/+
Rnaseh2a-/-
C
SP-9 pre-B cells
Myc-Pol m
Actin
Rnaseh2a-/- Polm-/-
+
Polm
D
SP-9 pre-B cells
TdT
Actin
Rnaseh2a-/- Polm-/-
+
Tdt
E
V(D)J Recombination Induction (fold over uninduced)
ns
ns
*
*
Rnaseh2a+/+ Polm+/+
Rnaseh2a-/- Polm+/+
Rnaseh2a-/- Polm-/-
+
Polm
+
Tdt

Fig. S4

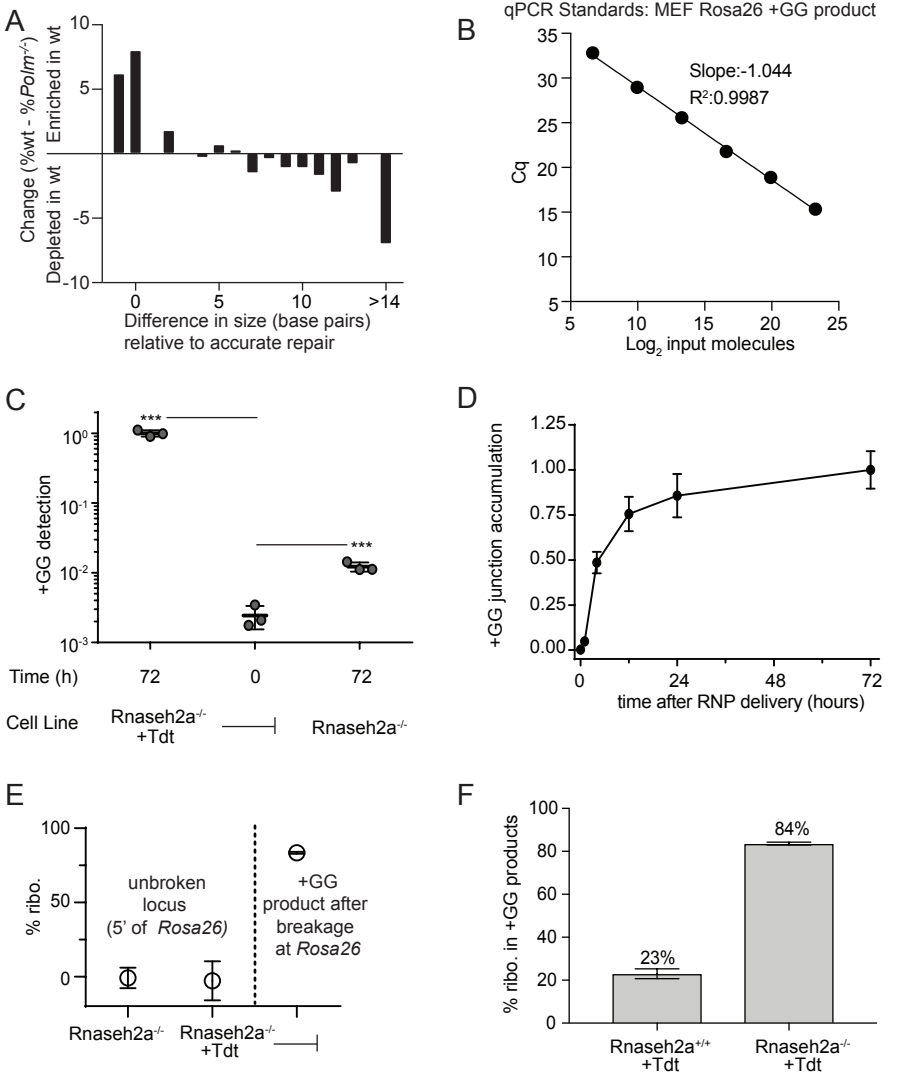
A
Change (%wt - %Polm-/-)
Enriched in wt
Depleted in wt
10
5
-5
-10
0
5
10
>14
Difference in size (base pairs)
relative to accurate repair
B
qPCR Standards: MEF Rosa26 +GG product
Slope:-1.044
R2:0.9987
Cq
35
30
25
20
15
10
5
5
10
15
20
25
Log2 input molecules
C
+GG detection
***
***
Time (h)
72
0
72
Cell Line
Rnaseh2a-/- +Tdt
Rnaseh2a-/-
D
+GG junction accumulation
1.25
1.00
0.75
0.50
0.25
0.00
0
24
48
72
time after RNP delivery (hours)
E
% ribo.
100
50
0
unbroken locus (5' of Rosa26)
+GG product after breakage at Rosa26
Rnaseh2a-/-
Rnaseh2a-/- +Tdt
F
% ribo. in +GG products
100
80
60
40
20
0
84%
23%
Rnaseh2a+/+ +Tdt
Rnaseh2a-/- +Tdt

Fig. S5

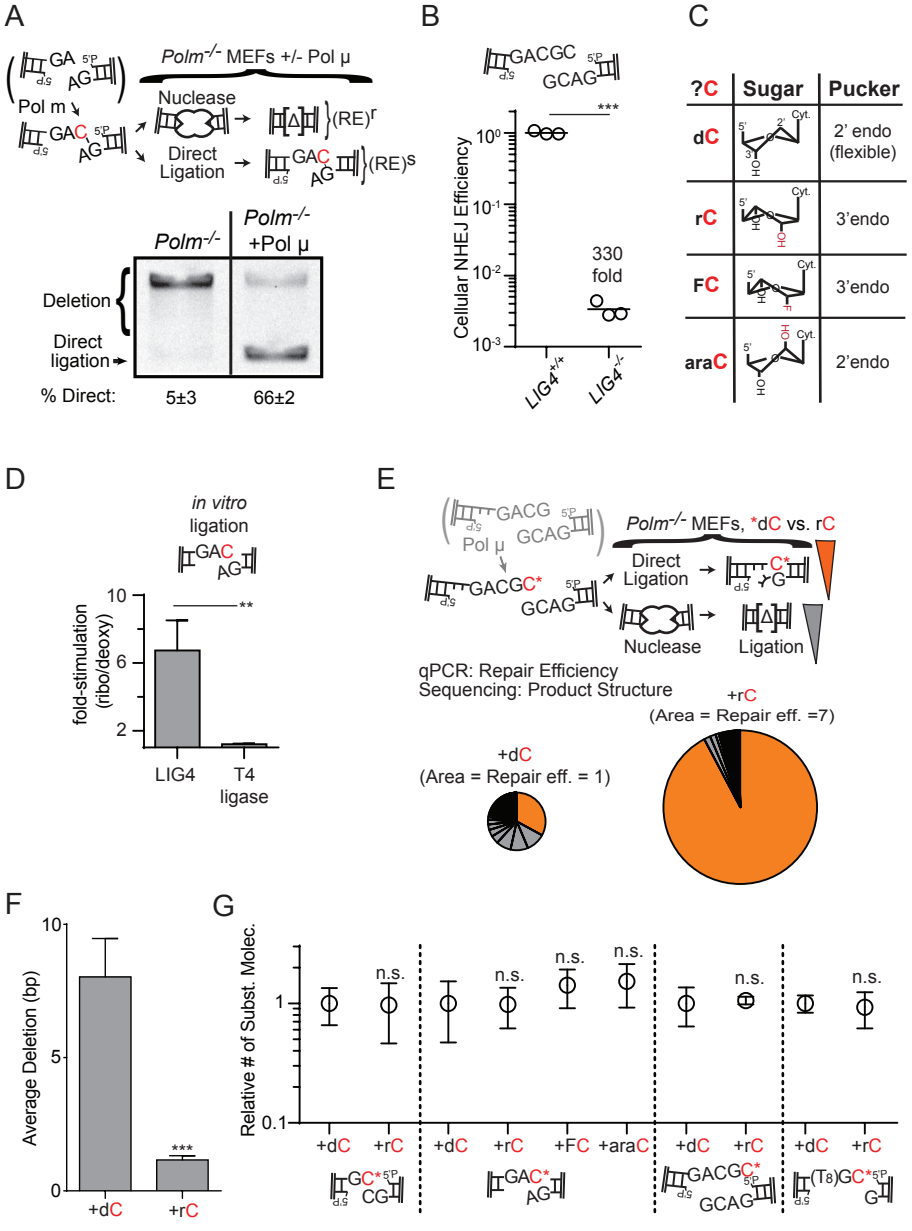
A
Polm-/- MEFs +/- Pol μ
Pol m
Nuclease
Direct Ligation
(RE)r
(RE)s
Polm-/-
Polm-/- +Pol μ
Deletion
Direct ligation
% Direct:
5±3
66±2
B
Cellular NHEJ Efficiency
330 fold
***
LIG4+/+
LIG4-/-
C
?C
Sugar
Pucker
dC
2' endo (flexible)
rC
3'endo
FC
3'endo
araC
2'endo
D
in vitro ligation
fold-stimulation (ribo/deoxy)
**
LIG4
T4 ligase
E
Polm-/- MEFs, *dC vs. rC
Pol μ
Direct Ligation
Nuclease
Ligation
qPCR: Repair Efficiency
Sequencing: Product Structure
+dC
(Area = Repair eff. = 1)
+rC
(Area = Repair eff. =7)
F
Average Deletion (bp)
***
+dC
+rC
G
Relative # of Substr. Molec.
n.s.
+dC
+rC
+FC
+araC

Fig. S6

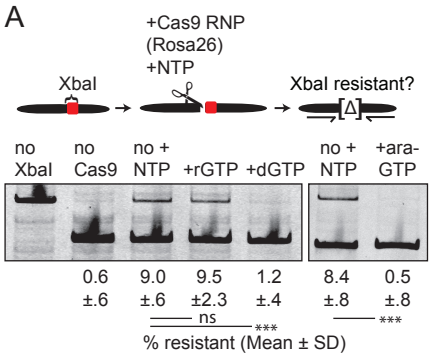
A
+Cas9 RNP
(Rosa26)
+NTP
XbaI
XbaI resistant?
[Δ]
no XbaI
no Cas9
no + NTP
+rGTP
+dGTP
no + NTP
+ara-GTP
0.6 ±.6
9.0 ±.6
9.5 ±2.3
1.2 ±.4
8.4 ±.8
0.5 ±.8
ns
***
***
% resistant (Mean ± SD)

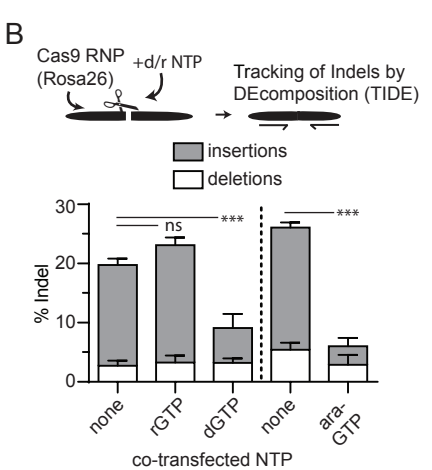
B
Cas9 RNP
(Rosa26)
+d/r NTP
Tracking of Indels by DEcomposition (TIDE)
insertions
deletions
% Indel
30
20
10
0
ns
***
***
none
rGTP
dGTP
none
ara-GTP
co-transfected NTP

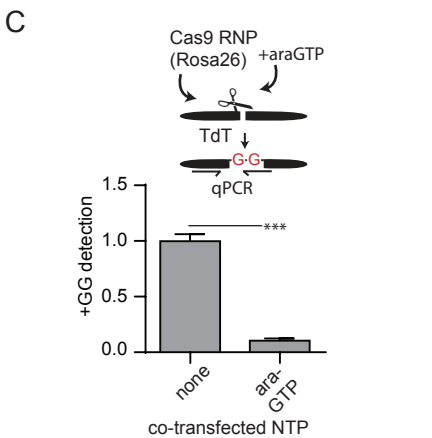
C
Cas9 RNP
(Rosa26)
+araGTP
TdT
G·G
qPCR
+GG detection
1.5
1.0
0.5
0.0
***
none
ara-GTP
co-transfected NTP